# General Disclaimer

## One or more of the Following Statements may affect this Document

- This document has been reproduced from the best copy furnished by the organizational source. It is being released in the interest of making available as much information as possible.

- This document may contain data, which exceeds the sheet parameters. It was furnished in this condition by the organizational source and is the best copy available.

- This document may contain tone-on-tone or color graphs, charts and/or pictures, which have been reproduced in black and white.

- This document is paginated as submitted by the original source.

- Portions of this document are not fully legible due to the historical nature of some of the material. However, it is the best reproduction available from the original submission.

NASA TM X-*65496*

# CURRENT SHEET MAGNETIC MODEL FOR THE SOLAR CORONA

## KENNETH H. SCHATTEN

MARCH 1971

**GSFC** —— **GODDARD SPACE FLIGHT CENTER** ——
**GREENBELT, MARYLAND**

CURRENT SHEET MAGNETIC MODEL FOR THE SOLAR CORONA

by

Kenneth H. Schatten
Laboratory for Extraterrestrial Physics
NASA-Goddard Space Flight Center
Greenbelt, Maryland

## Abstract

A new magnetic model is developed and compared with previous models
and the observed solar corona. An attempt is made to more accurately
compute the three dimensional currents flowing in the solar corona.
Physical reasons are given that require most of the large-scale currents
flowing in the solar corona to lie near thin sheets. The current sheets
are not constrained into any particular geometry or symmetry as in the
previous models of Altschuler and Newkirk (1969) and Schatten et al.
(1969). A comparison with the axisymmetric, isothermal MHD solution of
Pneuman and Kopp (1970) suggests that the model is able to simulate to
high accuracy an isothermal corona. A comparison of the model with the
May 30, 1965 solar eclipse and the November 12, 1966 solar eclipse shows
the model is capable of computing many features including the polar
plume  orientations as well as radial and non-radial streamers in the
solar corona.

## Introduction

The advent of large digital computers and detailed magnetograms has permitted sophisticated analyses of magnetic field configurations in the vicinity of the sun as suggested by Gold (1956). Computations of the coronal magnetic field utilizing potential theory began with the Schmidt (1964) program to plot current-free magnetic fields above active regions. Rust (1966) has compared the field configuration of the Schmidt program with direct observations of prominent material. Newkirk et al. (1968) utilized potential theory over the entire sun to calculate field patterns for a comparison with the projected appearance of the November 12, 1966 solar eclipse. Schatten (1968a,b) and Schatten et al. (1969) developed a "source surface" technique to calculate the effect of coronal currents upon the field. The currents were chosen to draw the field into a radial direction (Figure 1). This model allowed comparisons of fields calculated with the interplanetary field, a Faraday rotation coronal occulation experiment, and the projected appearance of many solar eclipse (see Schatten, 1968a, 1968b, 1969, 1970), Stelzried et al. (1970), and Smith and Schatten (1970)). The technique has received favorable review by Cowling (1969).

Schatten et al. (1969) utilized a "source surface" located at 0.6 solar radii above the photosphere. This distance was chosen from a parametric fit of this quantity based upon comparisons of the model with the observed interplanetary field. This would be the location in the model where the highest coronal loops would form. Bugoslavaskaya (1950) observed the solar corona from 1887 to 1945 and Newkirk (1967) found the highest closed arches have a mean height of 0.6 solar radii above the limb.

Further evidence for the highest closed magnetic loops lying near 0.6 solar radii above the limb is provided by the observations of Takakura (1966) that U bursts have a maximum height near this value. U bursts are thought to be essentially type III radio bursts caused by the motion of high speed

particles through the solar atomosphere, in which an increase in radio frequency emitted follows the usual decrease. The inversion in radio frequency emitted is interpreted as a decrease in altitude of these particles as they move through the corona on the magnetic field lines which govern their motion.

Although the magnetic models of the corona of Altschuler and Newkirk (1969) and Schatten et al. (1969) appear to be capable of calculating the large-scale structure of the coronal and interplanetary magnetic fields moderately well, there are several areas where notable deviations may be found that relate to the magnetic models. They are as follows:

1. Solar flares appear to affect the large-scale magnetic field of the corona. The influence may appear in a solar eclipse photograph as the formation of series of fine rays directed radially away from the source of the flare (Smith and Schatten, 1970).

2. Although much of the open field structures and closed field structures have the correct topology, the structures are not always directed properly. A notable example is the polar plumes. The plumes appear to bend continually equatorward, whereas the magnetic models orient them in the radial direction at the "source surface" or "zero potential surface". Another example are streamers. Their axes show a preferential lean to the equator near solar minimum and toward the poles at solar maximum (Waldmeier, 1970). Figure 2 illustrates the non-radial aspects of coronal features.

The first area of disagreement is expected due to the large amount of hot plasma emitted by a flare. The current-free assumption in the inner corona is violated by this hot plasma and thus the potential solution is no longer valid. The second area of disagreement may relate to the latitudinal and azimuthal magnetic pressure terms which are important in coronal structure but have been neglected beyond the zero potential surface in

prior work for mathematical simplicity. The purpose of this work will be
to improve the model by including this effect. The energy density of
the radial magnetic field (providing transverse pressure stresses) falls
off much less rapidly than that of the transverse field (see Schatten
et al. 1969). The energy density of the transverse field approximately
equals that of the plasma at about 0.6 solar radii (above the photosphere).
Thus the plasma extends the magnetic field outward near this point. In
the case of the radial field, equality with the plasma energy density is
only reached at the Alfven point near 25 solar radii. Thus transverse
magnetic pressure is expected to be an important effect long after the
coronal plasma has become supersonic. The magnetic field behaves like
open rigid wires along which the plasma is constrained to flow. The
magnetic field thus may still guide the plasma motion from 0.6 to 25 solar
radii. This paper suggests a method to mathematically calculate the
magnetic structure in this region.

Current Sheet Model

The value of $\beta$ (ratio of plasma to field energy density) for the
coronal plasma is significantly less than one out to the Alfven point.
Thus currents flowing in the coronal plasma cannot apply a significant
pressure on the magnetic field except where the field is weak (near regions
of opposite polarity fields). Currents are necessary to open the magnetic
field into sector-like structures. If any significant transverse currents
were located in regions of moderate field strength, a strong $\vec{j} \times \vec{B}$ force
would occur which the plasma could not resist. Thus the currents tend
to be present in high $\beta$ regions, where the field reverses, and the $\vec{j} \times \vec{B}$
forces are small. Thus the transverse currents flowing in the coronal
plasma in this model will be constrained to flow only where the field is
weak (near zero). This results in constraining the current to flow on

sheets near oppositely directed field regions. A mathematical way of
computing the location and strength of these current sheets is now developed.

The magnetic model suggested involves the use of current sheets as follows:
The magnetic field is first calculated directly from potential theory
using Legendre polynomial techniques, to a particular surface, a sphere
of radius 1.6 solar radii for example. Although not utilized in exactly
the same way, this sphere will again be referred to as the "source
surface". Following this, the magnetic field is reoriented such that it
points outward everywhere. However, the field is still along the same
direction and possesses the same field magnitude. Thus if $B_r \geq 0$ on this
"source surface" the field is unchanged but if $B_r < 0$, then $B_r$, $B_\theta$, and
$B_\phi$ are replaced by $-B_r$, $-B_\theta$ and $-B_\phi$. The field is then calculated beyond
the "source surface" from potential theory again using a Legendre
polynomial exansion of the field (see Appendix I). The difference being, that
now the monopole term is non-zero and rather large, thus it appears as if
the sun has a high magnetic monopole moment and all the Legendre polynomial
coefficients bear little or no relationship to their previous values
(see Figure 3). The effect of this physically is that beyond the "source
surface" the magnetic fields cannot now form closed arches as they are
all directed outward. This temporarily violates $\nabla \cdot \vec{B} = 0$ on the source
surface but this error will be corrected in a later step. This change of
field direction does not affect the magnetic stresses. They will remain
the same across the "source surface" and the field will still form a
minimum energy configuration (with the condition that the field lines
remain open). The last step (see Figure 4) is to revert the magnetic
field to its former sense of direction with the calculated strength
and orientation. This violates $\nabla \times \vec{B} = \frac{4\pi \vec{j}}{C} = 0$ unless appropriate current

sheets are introduced as shown.  Physically, current sheets are introduced

between areas of oppositely directed fields and thus prevent the field

from forming arches beyond the "source surface".  Note that the polar

fields and streamer fields possess similar shapes to those in the corona

(Figure 2) and not the radial orientation seen in Figure 1.

The invariance of the Maxwell stress tensor under this field reversal

scheme is important in order to insure against unequal stresses across

the "source surface".  The Maxwell stress tensor is defined such that

$\vec{j} \times \vec{B} = \nabla \cdot \overset{\leftrightarrow}{M}$.  The stress tensor is shown in Figure 5.  As can be seen,

changing the sign of the three components leaves $\overset{\leftrightarrow}{M}$ unchanged.  Thus the

magnetic stresses in the corona are balanced.

## Comparisons of the Current Sheet Model with Other Models and the Solar Corona.

The current sheet model is first compared with the "source surface"

and the "zero potential surface" models as well as an exact MHD solution

for an axisymmetric isothermal corona.  This latter solution has been

computed after the formalism of Pneuman and Kopp (1970) for the corona

with a temperature of $1.56 \times 10^6 \, ^\circ K$ and a dipole field.  Figure 6 shows this

comparison with an assumed dipolar solar field.  The field lines labelled

with crosses represent the present study with the "source surface" located

at 1.6 solar radii.  Solid lines indicate field directed away-from-the-sun

and dashed lines, field-toward-the-sun.  The heavy solid lines indicate the

MHD isothermal coronal solution of Pneuman and Kopp.  The dashed and

dotted lines indicate the field lines calculated by the Altschuler and

Newkirk model with a zero potential surface located at 2.5 solar radii.

The "source surface" solution of Schatten et al. (1969) is similar to this

solution except the field lines would be oriented radially somewhat closer

to the sun. As can be seen, the field lines computed from the isothermal
MHD solution and the current sheet solution are nearly identical. The
foot points of the field lines indicates the quality of their agreement.
The magnetic potential solution begins to diverge from the other solutions
near the zero potential surface. The rather close agreement between the
current sheet solution and the MHD solution suggests that much of the
current flowing in an isothermal corona does so near current sheets as
suggested earlier. Altschuler and Newkirk (1969) chose the location of the
zero potential sphere to be 2.5 solar radii based upon a comparison of
field geometry with coronal forms whereas Schatten et al. (1969) chose the
1.6 solar radii value for the "source surface" based upon the observed
highest closed arches and agreement with comparisons of their model with
the interplanetary magnetic field. In the present model, if the "source
surface" is set at 1.6 solar radii, the shapes of features are similar
(out to 2+ solar radii) with the Altschuler and Newkirk result and the
coronal magnetic field extends out from 1.6 solar radii, similar to the
result of Schatten et al. (1969). Thus the disagreement between these
two values where the coronal magnetic field extends outward may be ended
by utilizing this new model. The agreement with the axisymmetric MHD
solution suggests that the current sheet model may now be used with more
confidence in calculating fields in three dimensional non-symmetric
situations as well.

First, however, let us examine whether the current sheet model can
calculate non-radial streamers and compare them with observed non-radial
streamers. Figure 7 shows a drawing from Bohlin of the May 30, 1965 solar
eclipse from photographs by Smith (top). This eclipse shows, in addition
to the non-radial polar plumes, several non-radial streamers. The field

pattern beneath shows calculations from the current sheet model using an axisymmetric magnetic condition. As can be seen rather non-radial field lines may be computed in the model quite similar in appearance to the structures observed. The polar field lines appear similar to the polar plumes. The computed field configuration in the equatorial regions are also oriented toward the equator as in the eclipse drawing.

A computation of the magnetic field projected into the plane of the sky from this model for the November 12, 1966 solar eclipse is shown in Figure 8 superposed with a drawing of the coronal forms by Newkirk et al. (1970). The solid lines indicate away-from-the-sun magnetic field and dashed lines, toward-the-sun field. Many of the features line up surprisingly well with the field lines calculated as can be seen. Large-scale magnetic loops are calculated near streamers $\beta'$ and $\zeta$ and closed arches are observed underlying these streamers. Many of the "open" magnetic field lines near regions $\beta$, $\zeta$ and $\gamma$ are closely aligned with coronal features in the same areas. The general agreement of the magnetic field calculations with the observed features for this solar eclipse is rather good.

## Conclusions

A new current sheet magnetic model for the solar corona has been developed. It is capable of calculating the quiet large-scale magnetic field structure in the corona. As suggested by physical arguments, thin current sheets are utilized to separate regions of oppositely directed fields. This approximation appears to be a rather good one in that the dipole solution is nearly identical with the isothermal MHD coronal solution of Pneuman and Kopp.

A comparison of field computations with the observed structure for the May 30, 1965 solar eclipse reveals that the model appears to be capable of calculating the orientation of the polar plumes fairly well, as well as non-radial streamer configurations. A comparison between the computed magnetic field and the observed solar corona for the Nov. 12, 1966 solar eclipse is shown. Many of the observed features are also seen in the computed magnetic field.

## APPENDIX I

This appendix discusses the solution of the field beyond the "source surface" method of fitting the vector Legendre polynomial coefficients to the three dimensional vector field on the "source surface". The vector field up to and including the "source surface" is computed in accordance with the techniques of Altschuler and Newkirk (1969) without using any currents in the solar corona. The present model may be improved in the future by an iterative process using the currents computed in the present model to calculate the solution below the "source surface" as well and then recomputing the field beyond the "source surface". This may represent a minimum improvement, however.

The solution for the Laplacian equation in spherical coordinates is for $r \geq R$

$$\psi(r, \theta, \phi) = R \sum_{n=0}^{\infty} \sum_{m=0}^{n} \left[ \left( \frac{R}{r} \right)^{n+1} \left( g_n^m \cos[m\phi] + h_n^m \sin[m\phi] \right) P_n^m[\theta] \right] \quad (1)$$

The components of the magnetic field as as follows:

$$B_r = - \frac{\partial \psi}{\partial r} = f_1(g_n^m, h_n^m) \quad (2)$$

$$B_\theta = - \frac{\partial \psi}{r \, \partial \theta} = f_2(g_n^m, h_n^m) \quad (3)$$

$$B_\phi \quad = \quad - \quad \frac{1}{r \sin\theta} \quad \frac{\partial \psi}{\partial \phi} \quad = \quad f_3(g_n^m, h_n^m) \qquad (4)$$

The associated Legendre Polynomials utilizing the Schmidt normalization have been used (Chapman and Bartels, 1940). Thus in order to determine the magnetic field beyond the "source surface", it is necessary to compute $g_n^m$ and $h_n^m$ from the vector field on the "source surface" as a boundary condition.

The components of the magnetic field on the "source surface" are first oriented away-from-the sun so that if $B_r < 0$ on the "source surface", the signs of $B_r$, $B_\theta$, and $B_\phi$ are reversed.

In this analysis we have utilized a photospheric grid of 27 longitudes and 24 latitudes in equal steps of sinc (latitude). We have also chosen N=9 as the maximum principal Legendre index to consider for practical considerations. A "least mean square fit" to an overdetermined linear system of 1944(27x24x3) equations involving 100 unknowns is then utilized to best fit the fector field on the "source surface" as follows:

$$\text{Then let } F = \sum_{i=1}^{24} \sum_{j=1}^{27} \sum_{k=1}^{3} \left[ B(i,j,k) - f_k(g_n^m, h_n^m) \right]^2 \qquad (5)$$

where $B(i,j,k)$ equal the vector field components, where k=1, 2 or 3 refers to the radial, latitudial or azimuthal field component at $\theta_i$ and $\phi_j$.

It is necessary now to obtain $g_n^m$ and $h_n^m$ which minimize F, the sums of squares of the differences between the known components of the field on the "source surface", $B_r(i,j)$, $B_\theta(i,j)$ and $B_\phi(i,j)$, and the component

values computed from $g_n^m$ and $h_n^m$ at $\theta_i$ and $\phi_j$.

Let us choose

$$\alpha_{nm1} = (n+1) \cos m\phi \ P_n^m(\theta)$$

$$\beta_{nm1} = (n+1) \sin m\phi \ P_n^m(\theta)$$

$$\alpha_{nm2} = -\cos m\phi \ \frac{d}{d\theta} \ P_n^m(\theta)$$

$$\beta_{nm2} = -\sin m\phi \ \frac{d}{d\theta} \ P_n^m(\theta) \tag{6}$$

$$\alpha_{nm3} = \frac{m}{\sin \theta} \sin m\phi \ P_n^m(\theta)$$

$$\beta_{nm3} = \frac{m}{\sin \theta} \cos m\phi \ P_n^m(\theta)$$

Thus equation (5) becomes

$$F = \sum_i \sum_j \sum_k \ [B(i,j,k) - \sum_n \sum_m \ (g_n^m \ \alpha nmk + h_n^m \ \beta nmk)]^2 \tag{7}$$

The equations to minimize F are:

$$\frac{\partial F}{\partial g_n^m} = 0 \qquad \frac{\partial F}{\partial h_n^m} = 0 \tag{8}$$

for each (n, m) may be rewritten:

$$\sum_i \sum_j \sum_k \left\{ B(i,j,k) \ \alpha_{nmk}(ij) - \alpha_{nmk}(ij) \sum_{t=0}^{N} \sum_{s=0}^{t} [g_t^s \alpha_{tsk}(ij) + h_t^s \beta_{tsk}(ij)] \right\} = 0 \tag{9}$$

$$\sum_i \sum_j \sum_k \left\{ B(i,j,k)\beta_{nmk}(ij) - \beta_{nmk}(ij) \sum_{t=0}^{N} \sum_{s=0}^{t} [g_t^s \alpha_{tsk}(ij) + h_t^s \beta_{tsk}(ij)] \right\} = 0 \tag{10}$$

where t and s are dummy indices sued for n and m. The unknowns are $g_n^m$ and $h_n^m$ and B(i,j,k) is the known vector field and $\alpha$ and $\beta$ are known from equation 6.

Defining the following column vectors

$$\bar{\alpha}_{NM} = \begin{bmatrix} \alpha_{\theta_1\phi_1 1} \\ \alpha_{\theta_1\phi_2 1} \\ \vdots \\ \alpha_{\theta\phi 1} \\ \alpha_{\theta_1\phi_1 2} \\ \vdots \\ \alpha_{\theta\phi 3} \end{bmatrix}$$

$$\bar{\beta}_{NM} = \begin{bmatrix} \beta_{\theta_1\phi_1 1} \\ \beta_{\theta_1\phi_2 1} \\ \vdots \\ \beta_{\theta\phi 1} \\ \beta_{\theta_1\phi_1 2} \\ \vdots \\ \beta_{\theta\phi 3} \end{bmatrix}$$

is a column vector of length 24x27x3 for each NM.

(11)

and $\bar{B} = \begin{bmatrix} B(\theta_1,\phi_1,1) \\ B(\theta_1,\phi_2,1) \\ \vdots \\ B(\theta,\phi,1) \\ B(\theta_1,\phi_1,2) \\ \vdots \\ B(\theta,\phi,3) \end{bmatrix}$

and $\overline{GH} = \begin{bmatrix} g_0^0 \\ g_1^0 \\ g_1^1 \\ \vdots \\ g_N^N \\ h_1^1 \\ h_2^1 \\ \vdots \\ h_N^N \end{bmatrix}$

Now defining the matrix $\alpha\beta$ such that the rows of $\alpha\beta$ are as follows:

$$\alpha\beta(1) = \alpha_{00}$$
$$\alpha\beta(2) = \alpha_{10}$$
$$\alpha\beta(3) = \alpha_{11}$$
$$\cdots$$
$$\alpha\beta(55) = \alpha_{99}$$
$$\alpha\beta(56) = \beta_{11}$$
$$\cdots\cdots$$
$$\alpha\beta(100) = \beta_{99}$$

with all m = 0 elements missing from $h_n^m$ and from $\beta$. $\overline{GH}$ is a 100x1 matrix
and $\alpha\beta$ is a 100x1944 matrix. Equations (9) and (10) may be rewritten
as follows:

$$A\beta \cdot \overline{B} = AB \cdot \overline{GH} \tag{12}$$

choosing $AB(i,j) = \alpha\beta(i) \cdot \alpha\beta(j)$

so that $\alpha\beta$ is a 100x1944 matrix, $\overline{B}$ is a 1944x1 matrix, $AB_{ij}$ is a 100x100
matrix and $\overline{GH}$ is a 100x1 matrix.

By an inversion of the symmetric matrix AB, GH may be solved as follows:
$$\overline{GH} = AB^{-1} \cdot \alpha\beta \cdot \overline{B}$$

This requires inverting a square matrix each of whose sides equals $(N+1)^2$
which for N=9 is 100. This provides us with estimates for $g_n^m$ and $h_n^m$
which arise from a least mean square fit to the three vector components
of the magnetic field on the source surface. Equations (2), (3), and (4)
allow a compution of the magnetic field everywhere above the "source surface".
It is required, however, to reverse the sense of the three components of
the magnetic field depending upon whether the footpoint of the field
line has had its sense reversed (i.e. - if $B_r$ <0). Those field lines are
indicated by being drawn dashed.

## REFERENCES

Atschuler, M. D., and G. Newkirk, Jr., Magnetic fields and the structure of the solar corona, Solar Physics, 9, 131, 1969.

Bugoslavaskaya, E. Ya., Trud. Gos. Astronom. Inst. in Shternberga, 19, 3, 1950.

Cowling, T. G., The solar wind, The Observatory, 89, 217, 1969.

Gold, T., The magnetic field in the corona, IAU Symp. No. 6, 275, 1956.

Newkirk, G. A., Jr., Ann. Rev. Astron. and Astrophys. 5, 213, 1967.

Newkirk, G. A., Jr., M. D. Altschuler, and J. W. Harvey, Influence of magnetic fields on the structure of the solar corona: in Structure and Development of Solar Active Regions (ed. by K. O. Kiepenheuer) I.A.U. Symp. No. 35, D. Reidel Publ. Co., Dordrecht, p.379, 1968.

Newkirk, G. A., Jr., E. Schmahl, and R. Deupree, Magnetic fields and the structure of the solar corona II: observations of the 12 November 1966 solar eclipse, Solar Physics, 15, 15, 1970.

Pneuman, G. W., and R. A. Kopp, Coronal streamers III: Energy transport in streamer and interstreamer regions, Solar Physics, 13, 176, 1970.

Rust, D. M., Measurements of the magnetic fields in quiescent solar prominences, Ph.D. thesis, University of Colorado, 1966.

Schatten, K. H., Large-scale configuration of the coronal and interplanetary magnetic field, Thesis, University of California, Berkeley, 1968a.

Schatten, K. H., Prediction of the coronal structure for the solar eclipse of September 22, 1968, Nature, 220, 1211, 1968b.

Schatten, K. H., Coronal structure at the solar eclipse of September 22, 1968, Nature, 223, 652, 1969.

Schatten, K. H., J. M. Wilcox and N. F. Ness, A model of coronal and interplanetary magnetic fields, Solar Physics, 9, 442-455, 1969.

Schatten, K. H., Prediction of the coronal structure for the solar eclipse of March 7, 1970, Nature, 226, 251, 1970.

Schmidt, H. U., On the observable effects of magnetic energy storage and release connected with solar flares, in AAS-NASA Symp. Phys. Solar Flares, ed. W. N. Hess, NASA-SP-50, p.107, 1964.

Smith, S. M., K. H. Schatten, Nature, 226, 1130, 1970.

Stelzried, C. T., G. S. Levy, T. Sato, W. V. T. Rusch, J. E. Ohlson, K. H. Schatten, and J. M. Wilcox, Solar Physics, 14, 440, 1970.

Takakura, T.: Space Science Reviews, 5, 80, 1966.

Waldmeier, M., Nature, 226, 1131, 1970.

## FIGURE CAPTIONS

Figure 1    Magnetic field geometry in the "source surface" or "zero
            potential surface" models. The fields are constrained to the
            radial direction by the solar wind in these models. The
            equations obeyed in the different regions are shown.

Figure 2    Drawing of the Feb. 15, 1961 solar eclipse (top) and the
            Feb. 25, 1952 solar eclipse (bottom) superposed with a
            "source surface" at 1.6 solar radii. Note that most closed
            arches fall below this surface. Beyond this distance most
            structures are "open" but not strictly radially oriented.

Figure 3    First step in the current sheet magnetic model. A potential
            solution is derived for the field between the "source
            surface" and the photosphere. The field computed on the
            source surface is then reoriented so that it points outward
            everywhere. The field is then computed beyond the "source
            surface" from potential theory. The sense of the magnetic
            field is opposite half the time to what it should be. This
            "error" is corrected in the next step.

Figure 4    Second step in the current sheet magnetic model. The field
            that was disoriented is reoriented by reversing the sense
            of the magnetic field components. This requires a current
            sheet to be employed in the corona to separate regions of
            oppositely directed field to obey Maxwell's equations.
            Allowing the magnetic field to "open" by thin current  sheets
            is consistent with the physical model of this region of
            the corona possessing a low $\beta$. If significant

transverse currents flowed elsewhere a strong $\vec{j} \times \vec{B}$
force would develop which the plasma could not maintain. This
model may be used to calculate the magnetic oriented structures
in the corona with less simplified solar wind currents.

Figure 5     The Maxwell stress tensor. Note that it is identical if
all three components are reversed. This allows the stresses
to be balanced after the field reversal processes.

Figure 6     A comparison of solutions for a dipole solar field with
the zero potential surface model (Altschuler and Newkirk),
the present model and the exact isothermal MHD coronal
solution (Pneuman and Kopp). Note that the present solution
is quite similar to the isothermal coronal solution supporting
the suggestion that the coronal currents are confined to
thin sheets.

Figure 7     A comparison of the structure of the solar corona during
the May 30, 1965 solar eclipse (top) with computions from
an assumed axisymmetric photospheric field pattern (bottom).
The shape of the polar plumes is calculated quite well in
this model as well as a non-radial helmet streamer.

Figure 8     A comparison of the computed coronal magnetic field with
a drawing of the solar eclipse features from Newkirk and
Altschuler (1970) for the Nov. 12, 1966 solar eclipse.
The solid lines represent magnetic field directed away-from-
the-sun and the dashed lines field toward-the-sun. The
field lines originate on the photosphere in the center of
each of the 648 grid points. Many of the observed features

line up with the computed field lines.  The computed

field lines terminate at five solar radii and are projected

into the plane of the sky.

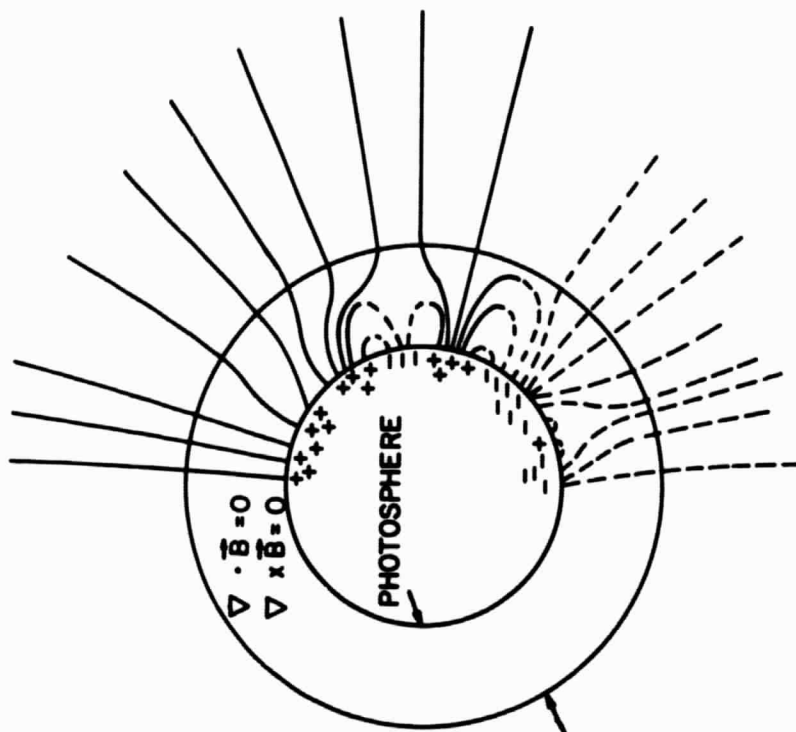$$\nabla \times \vec{B} = \frac{4\pi \vec{j}}{c}$$

$$\nabla \cdot \vec{B} = 0$$

$$B_\theta = 0$$

$$B_\phi = 0$$

$$j \neq 0$$

$$\nabla \cdot \vec{M} \neq 0$$

"SOURCE SURFACE" OR ZERO POTENTIAL SURFACE

$$\nabla \cdot \vec{B} = 0$$

$$\nabla \times \vec{B} = 0$$

PHOTOSPHERE

"SOURCE SURFACE" OR ZERO POTENTIAL SURFACE

—— OUTWARD MAGNETIC FIELD

---- INWARD MAGNETIC FIELD

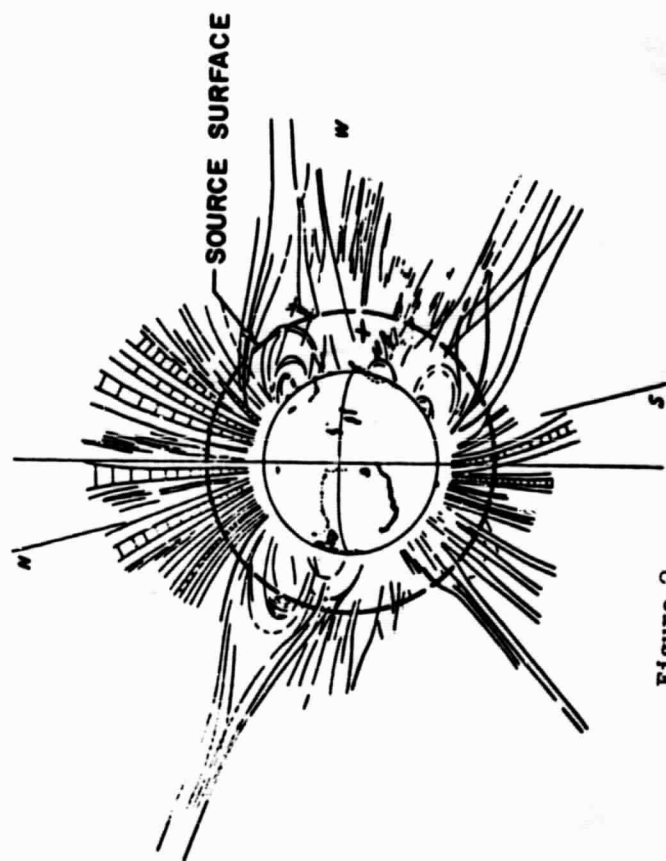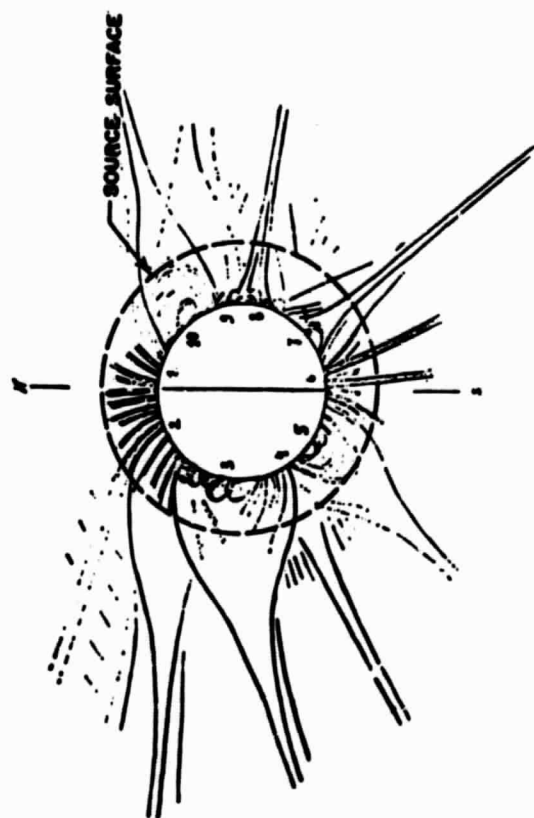"SOURCE SURFACE" OR ZERO POTENTIAL SURFACE MODELS

Figure 1

Figure 2

Figure 3

SOURCE SURFACE
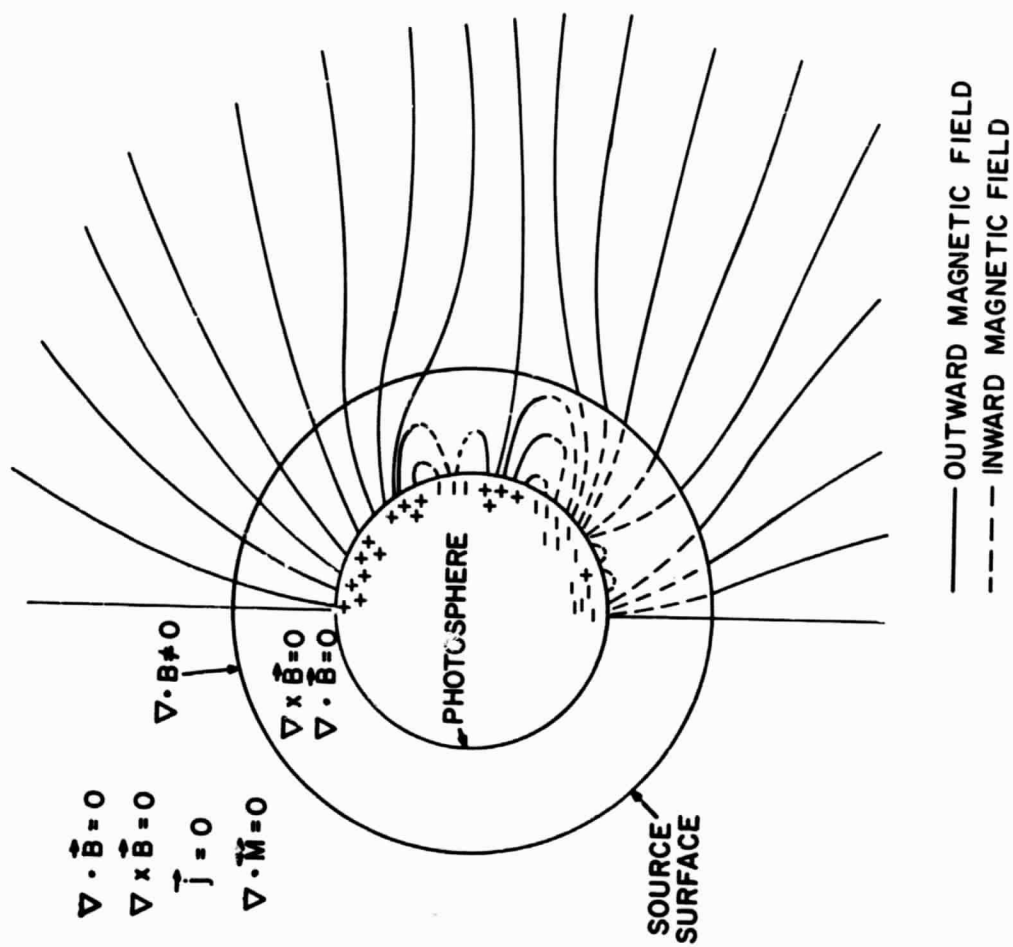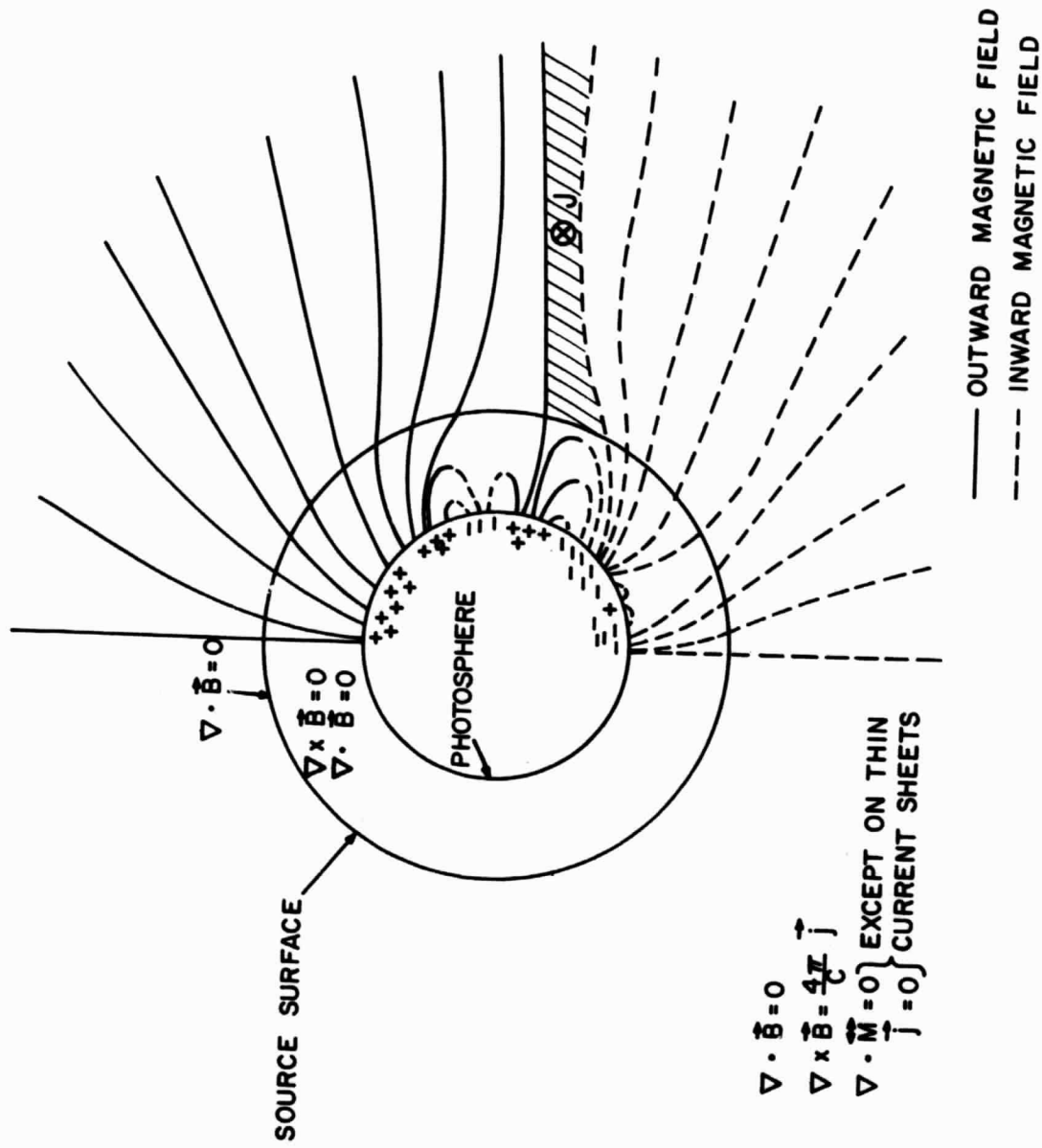
$\nabla \cdot \vec{B} = 0$

PHOTOSPHERE

$\nabla \times \vec{B} = 0$
$\nabla \cdot \vec{B} = 0$

$\nabla \cdot \vec{B} = 0$

$\nabla \times \vec{B} = \dfrac{4\pi}{c} \vec{j}$

$\nabla \cdot \vec{M} = 0$
$\vec{j} = 0$ } EXCEPT ON THIN
CURRENT SHEETS

———— OUTWARD MAGNETIC FIELD
-------- INWARD MAGNETIC FIELD

Figure 4

$$\vec{j} \times \vec{B} = \nabla \cdot \overleftrightarrow{M}$$

$$\overleftrightarrow{M} = \frac{1}{\mu_0} \begin{bmatrix} \frac{1}{2}(B_X^2 - B_Y^2 - B_Z^2) & B_X B_Y & B_X B_Z \\ B_X B_Y & \frac{1}{2}(B_Y^2 - B_X^2 - B_Z^2) & B_Y B_Z \\ B_X B_Z & B_Y B_Z & \frac{1}{2}(B_Z^2 - B_X^2 - B_Y^2) \end{bmatrix}$$
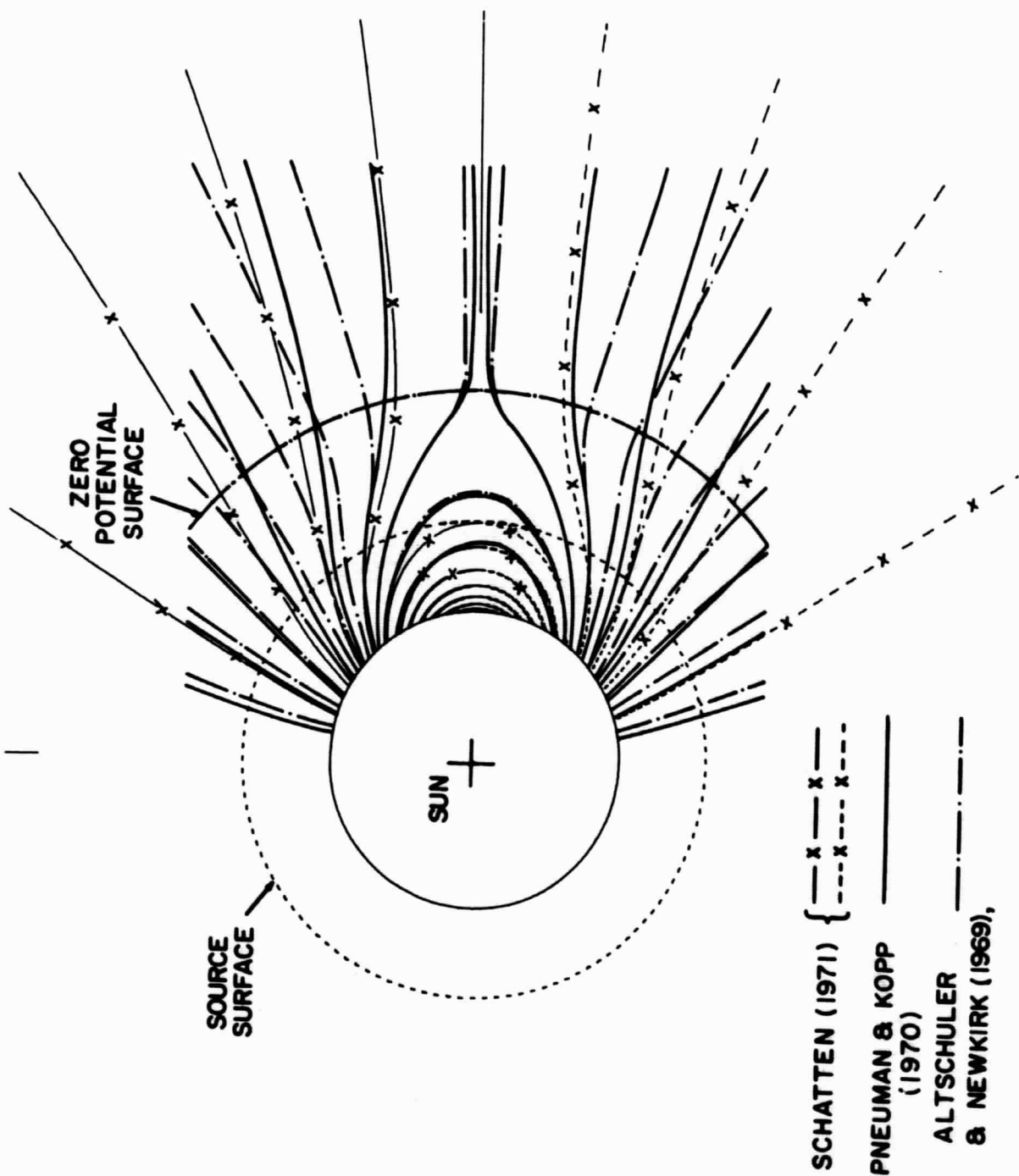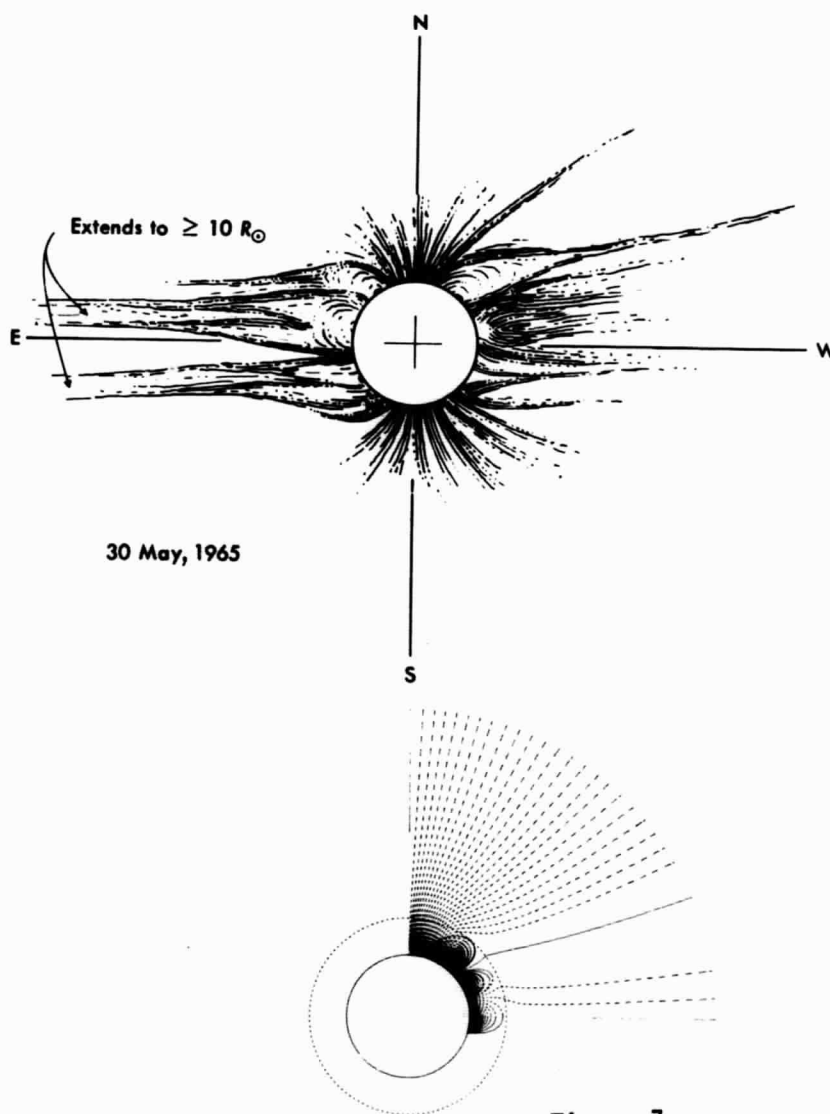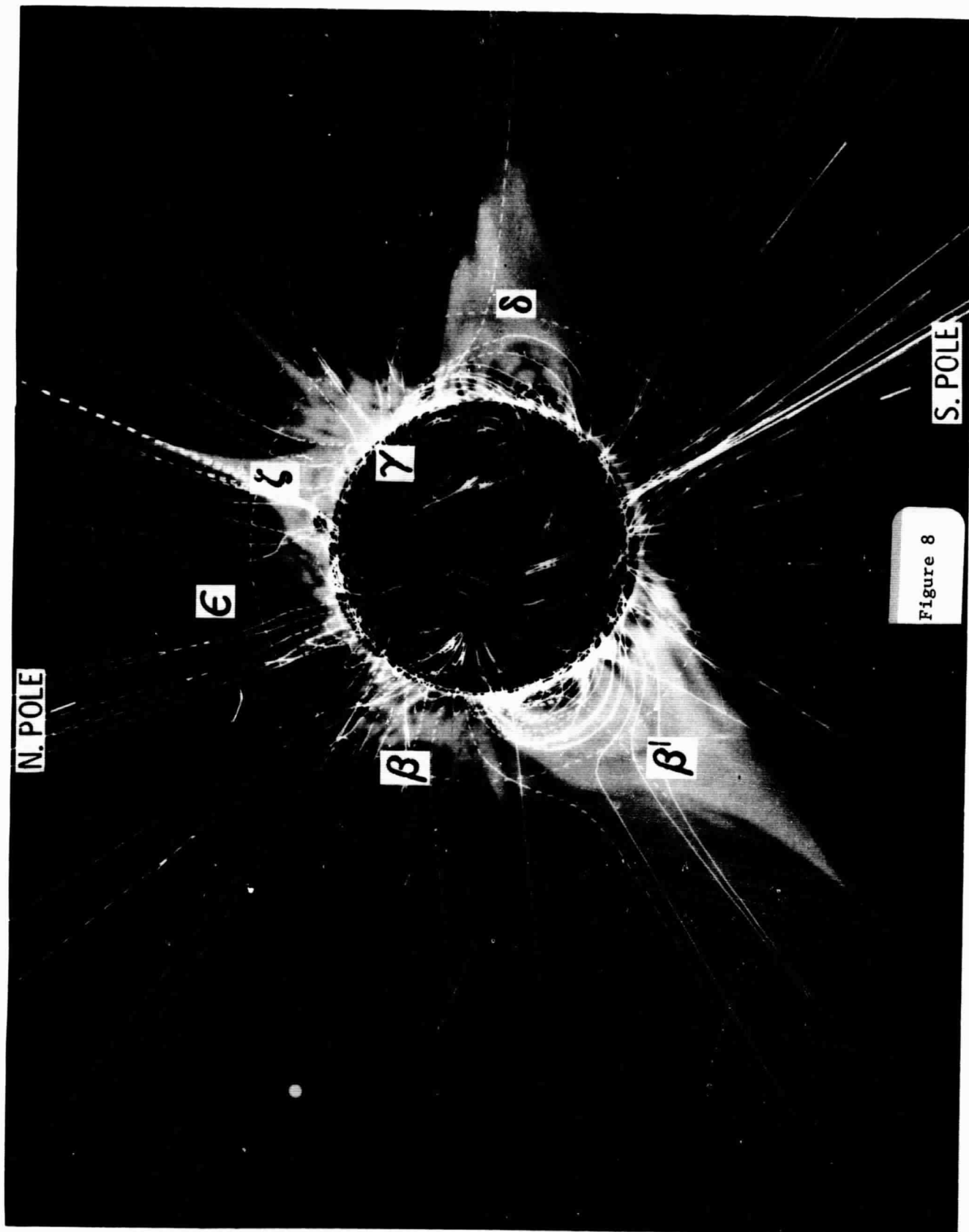
Figure 5

ZERO POTENTIAL SURFACE

SOURCE SURFACE

SUN

SCHATTEN (1971)
PNEUMAN & KOPP (1970)
ALTSCHULER & NEWKIRK (1969),

Figure 6

Extends to $\geq 10\ R_\odot$

30 May, 1965

Figure 7

N. POLE

S. POLE

δ

ζ

γ

ε

β

β'

Figure 8